

Strong Electron-Hole Exchange in Coherently Coupled Quantum Dots

Stefan Fält,¹ Mete Atatüre,² Hakan Tureci,¹ Yong
Zhao,³ Antonio Badolato,¹ and Atac Imamoglu¹

¹*Institute of Quantum Electronics, ETH Zurich, 8093 Zurich, Switzerland*

²*Cavendish Laboratory, University of Cambridge,
Cambridge, CB3 0HE, United Kingdom*

³*Physikalisches Institut, Ruprecht-Karls-Universität Heidelberg,
Philosophenweg 12, 69120 Heidelberg, Germany*

(Dated: October 31, 2018)

Abstract

We have investigated few-body states in vertically stacked quantum dots. Due to small inter-dot tunneling rate, the coupling in our system is in a previously unexplored regime where electron-hole exchange is the dominant spin interaction. By tuning the gate bias, we are able to turn this coupling off and study a complementary regime where total electron spin is a good quantum number. The use of differential transmission allows us to obtain unambiguous signatures of the interplay between electron and hole spin interactions. Small tunnel coupling also enables us to demonstrate all-optical charge sensing, where conditional exciton energy shift in one dot identifies the charging state of the coupled partner.

Self-assembled quantum dots (QDs) are semiconductor nanostructures that exhibit three-dimensional confinement of carriers. Due to spatial confinement, the electronic states in a QD are quantized and these structures have been referred to as artificial atoms. This description has been demonstrated experimentally with atom-like properties such as strong photon antibunching [1] and near life-time limited linewidths [2]. One can use the self-assembly mechanism to create aligned nanostructures that function as QD molecules. Earlier studies have demonstrated hybridization of energy levels of two coupled QDs [3], spectral signatures of tunnel coupling of multiple-hole [4, 5] or two-electron [6] states. It has also been shown that the g-factor can be engineered with control of the tunneling [7]. In contrast to the previously well studied coupling regime [6], in our system the inter-dot electron coupling mechanism is significantly modified by electron-hole exchange. By tuning the gate bias, the complementary regime of pure electron-electron exchange was also investigated. Here, we use resonant scattering techniques to resolve the spectral signatures of various coupling mechanisms. We studied the optical emission and absorption from both QDs in the pair, which allowed us to use inter-dot Coulomb interactions in the system to determine the charging state of both QDs.

The heterostructures for the device for this work was grown with molecular beam epitaxy on a GaAs substrate. The sample consists of two layers of QDs, separated with 15 nm of GaAs, in a diode structure. The back contact consists of a n-doped layer and the top contact is a semi-transparent layer of Ti. The QD layer close to the back contact was separated from it with 25 nm GaAs and more blue-shifted than the layer closer to the top contact. The layers will be referred to as the blue and red layers, respectively. The red layer was spaced from the top gate with 160 nm GaAs, including an AlGaAs current blocking layer close to the top gate. The strain field on top of QDs from the blue layer gives a natural alignment of the nucleation of QDs in the red layer so that stacks are formed.

The measurements were performed using micro-photoluminescence (μ -PL) and differential transmission (DT) techniques at 4.2 K. For μ -PL, a 780 nm laser was used to create free carriers in the bulk GaAs. A lens with NA of 0.55 was used to both focus this laser and collect the luminescence, which was spectrally resolved with a resolution of 30 μ eV. For DT measurements, a single frequency laser was tuned across the coupled QD resonances. A Si p-i-n photodiode detected the transmitted laser light and a lock-in amplifier was used with Stark-shift modulation of the resonances to eliminate low frequency noise [8].

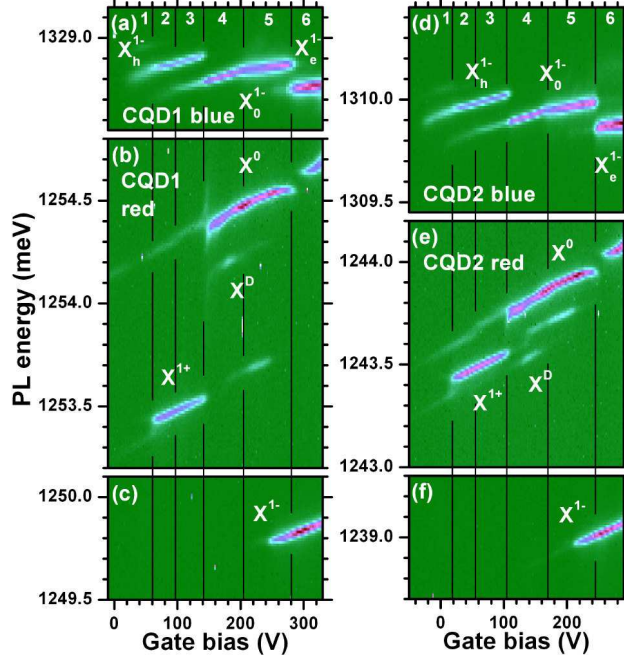


FIG. 1: PL plots of two different pairs of stacked QDs as a function of the applied gate bias where (a) and (d) show PL data from the blue QDs of the pair, (b), (c), (e), and (f) show the data from the red QDs. The PL lines are identified with the corresponding excitonic states. Regions with different charge combinations are separated with black vertical lines and numbered. Using the notation (B, R) , where B denotes the ground state charge of the blue QD and R that of the red QD, the ground state charge configurations are: 1: $(0, 0)$ or $(0, h^+)$, 2: $(0, 0)$ or (e^-, h^+) , 3: $(e^-, 0)$ or (e^-, h^+) , 4: $(e^-, 0)$, 5: $(2e^-, 0)$ and 6: $(2e^-, e^-)$.

The diode structure allows controlled electron charging of the QDs. As the stacking probability of the QDs is not unity, we were able to use single QDs without a coupled partner to investigate the spectral signatures of charging in the absence of coupling. These QDs showed no fundamental differences from what is known about single QDs in charge-injection devices. The charging behavior changes with the potential well depth, but also with the distance to the doped layer. In addition to emission wavelength, this difference in charging behavior between the layers aids us in the identification of which layer a certain QD is in.

The relatively large tunnel barrier between our dots allows us to study the emission properties of each QD of a pair with μ -PL. In Figure 1, we present data from two pairs of coupled QDs (CQD1 and CQD2), focusing on three separate PL energy windows in the same gate voltage range. Figures 1 (a) and (d) show the PL intensity lines of the negatively

charged trion on the blue dot. Figures 1 (b) and (e) contain the the lines for the neutral bright exciton (X^0), dark exciton (X^D) and positively charged trion (X^{1+}), while Figures 1 (c) and (f) show the negatively charged trion (X^{1-}) lines [9] for the red QDs. We first note that the X^{1-} line of the blue QDs in Figures 1 (a) and (d) is split into three, following closely the charging state of their partners in Figures 1 (b) and (e) respectively. In other words, the wavelength of the X^{1-} line of the blue QDs is conditional on the ground state of its red partner. We indicate this using the following notation: X^{1-} for a single hole charge (X_h^{1-}), neutral (X_0^{1-}) and single electron charge (X_e^{1-}) on the red dot. The measured splittings between regions 5 and 6 ($110 \mu\text{eV}$) and 3 and 4 ($130 \mu\text{eV}$) is consistent with the estimated dipole shifts of the order of $100 \mu\text{eV}$ extracted from the dc Stark shift of the lines. We note here that the shifts of the lines *in the red QD* due to charge sensing in comparison is smaller and in the opposite direction. While the latter observation is easily explained by the charge being on the opposite side of the dipole as compared to the case of the blue QD, the latter indicates a different spatial composition of the red QD due to the strain field of their partners in the first layer. This possibility is consistent with the X^{1+} line being red-shifted as compared to the neutral exciton in contrast to previous reports on single-dots [10].

In order to investigate the spin fine structure in the regions 3 and 4, we now focus on the DT measurements which provide higher resolution and eliminate spurious effects associated with the generation of free charges in the bulk GaAs. Figures 2(a) and 2(b) show data from the DT measurements carried out at zero external magnetic field on the blue and red QD, respectively. The blue QD shows a splitting due to the charge sensing that we noted earlier in the PL data. At 205 mV gate bias when the blue dot charging changes, we see a kink in the red QD DT signal; at present, we do not understand this feature. Figure 2(c) shows the counterpart of Fig. 2(b) with an applied magnetic field 0.4 T in Faraday configuration [15]. In these plots, the QDs are in the gate bias regime where we see X^{1-} absorption in the blue QD and X^0 absorption in the red QD. Based on the DT data shown and the unambiguous identification of the charging states through charge sensing, we can with very high confidence state that the excited states we probe in the DT measurements of Fig. 2(b) involve one hole localized in the red QD and two electrons. The DT signal disappears below a gate voltage of 150 mV, due to the fact that one of the optically generated electrons become unstable and tunnels out in to the free electron gas: in this regime, the red QD can be optically charged with a hole.

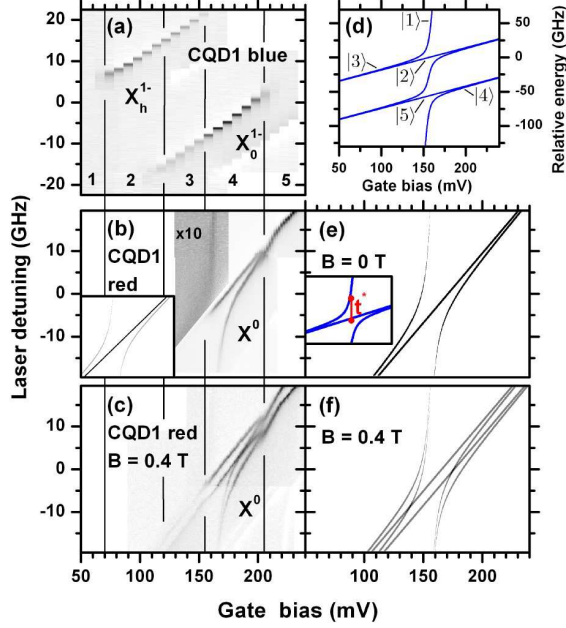


FIG. 2: (a) DT measurements showing two split lines for the blue X^1- due to charge sensing. Charges can be introduced into the red QD in this case due to excitation to higher excited state configurations. (b) DT measurements on the red X^0 and (c) red X^0 in an external magnetic field of 0.4 T. (d) Calculated optically excited state level diagram as a function of gate bias. Calculated absorption (e) without and (f) with magnetic field. The inset to (b) shows the expected absorption for vanishing electron-hole exchange. The inset to (e) indicates the definition of the coupling strength t^* in our system.

The results shown in Figs. 2(b-c) indicate a different regime of coherent coupling from those realized in previous studies on CQDs [6], where electron-electron exchange was found to dominate the spin interactions. This can be seen most notably in the ratio of the transition strengths of the anti-crossing and crossing branches in Fig. 2(b) which here is about 1:1 as opposed to 1:3 in previous studies (for comparison, a numerical calculation for that regime is provided in the inset to Fig. 2(b)). Based on a simple model that we present below, we attribute this qualitative difference to an unusually strong intra-dot electron-hole exchange interaction. We find that the following basis most transparently describes the DT data

$$\begin{aligned}
 |1\rangle &= e_{B\downarrow}^\dagger e_{B\uparrow}^\dagger h_{R\uparrow}^\dagger |0\rangle = (\downarrow\uparrow, \uparrow), & |6\rangle &= (\downarrow\uparrow, \downarrow), \\
 |2\rangle &= e_{B\downarrow}^\dagger e_{R\downarrow}^\dagger h_{R\uparrow}^\dagger |0\rangle = (\downarrow, B_+), & |7\rangle &= (\downarrow, B_-),
 \end{aligned}$$

$$\begin{aligned}
|3\rangle &= e_{B\uparrow}^\dagger e_{R\downarrow}^\dagger h_{R\uparrow}^\dagger |0\rangle = (\uparrow, B_+), & |8\rangle &= (\uparrow, B_-), \\
|4\rangle &= e_{B\downarrow}^\dagger e_{R\uparrow}^\dagger h_{R\uparrow}^\dagger |0\rangle = (\downarrow, D_+), & |9\rangle &= (\downarrow, D_-), \\
|5\rangle &= e_{B\uparrow}^\dagger e_{R\uparrow}^\dagger h_{R\uparrow}^\dagger |0\rangle = (\uparrow, D_+), & |10\rangle &= (\uparrow, D_-),
\end{aligned}$$

here, $e_{i\sigma}^\dagger$ ($h_{i\sigma}^\dagger$) creates a spin- σ electron (hole) in the blue ($i = B$) or red ($i = R$) dot (\uparrow, \downarrow refer to the hole pseudo-spin $J_z = \pm 3/2$). The states $|1\rangle$ and $|6\rangle$ forms a spin singlet with both electrons in the blue QD and the other states are compositions of the one electron in the blue QD with a certain spin and a bright (B_\pm) or dark (D_\pm) exciton in the red QD, where " \pm " refers to right-hand/left-hand circular polarization. Considering the states from $|1\rangle$ to $|5\rangle$, relevant for DT measurements carried out using right-hand circularly polarized laser, the Hamiltonian for this system and basis states is:

$$\begin{pmatrix}
d_i \frac{V}{l} + U & 0 & t_e & -t_e & 0 \\
0 & E_1 & 0 & 0 & 0 \\
t_e & 0 & E_1 & 0 & 0 \\
-t_e & 0 & 0 & E_2 & 0 \\
0 & 0 & 0 & 0 & E_2
\end{pmatrix}$$

where $E_1 = \frac{1}{2}\delta_0 + d_d \frac{V}{l}$, $E_2 = -\frac{1}{2}\delta_0 + d_d \frac{V}{l}$, V is the applied gate bias, l is the distance between the back and top gates, d_i and d_d are the sizes of effective indirect and direct static dipoles and U is the intra-dot Coulomb interaction for two electrons in the blue QD measured with respect to their inter-dot Coulomb interaction. We consider a Hamiltonian that is extended in block diagonal form when we consider all 10 states as we can neglect the anisotropic electron-hole exchange interaction [16]. Simulations has been carried out with the extended 10 state Hamiltonian and an energy level diagram as a function of gate bias V for typical parameters is given in Fig. 2(d) with only states $|1\rangle$ to $|5\rangle$ labeled. The calculated DT absorption spectra are shown in Fig. 2(e) ($B = 0$) and 2(f) ($B = 0.4T$). The applied magnetic field lifts the degeneracy of the different electron-hole spin configuration. An important feature of this Hamiltonian is the coupling of the state $|1\rangle$ with the states $|3\rangle$ and $|4\rangle$ through the t_e term, and as shown in Fig. 2(d). This particular hybridization will brighten the dark exciton $|4\rangle$ in a narrow gate bias regime around the anti-crossing as seen in the PL data of Fig. 1(b) and (e) (Line marked X^D). Note that the X^D is brightest at a

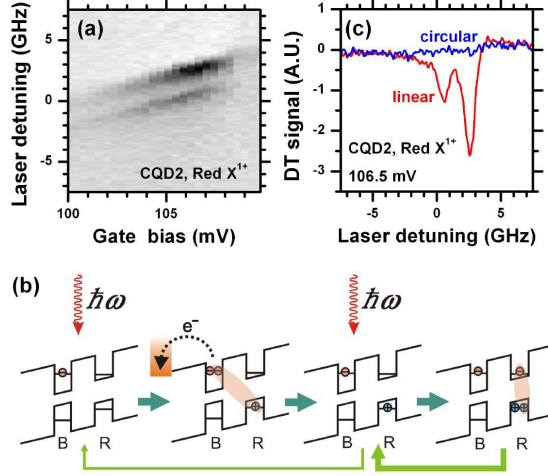


FIG. 3: (a) DT measurements of X^+ with excitation of only one laser. (b) Schematic description of the two-photon process resulting in scattering of the X^{1+} transition with only one resonant laser (c) Polarization dependence of the X^+ line, showing maximum absorption of linearly polarized light and minimal for circularly polarized light.

somewhat larger gate bias than predicted.

By fitting our model to the PL and DT data, we determine the isotropic part of electron-hole exchange interaction δ_0 in the red QD of CQD1 to be $230\mu eV$, while the single electron coupling is estimated to be $t_e = 137\mu eV$, indicating we are in a new regime where the intra-dot electron-hole exchange interaction is the dominant scale. The strength of the anti-crossing considered ($t^* = 161\mu eV$ indicated in the inset of Fig. 2(e)) implies that the exchange interaction is mainly mediated by *one* electron tunneling, while in the typical case of weak electron-hole exchange the value is about $t^* = \sqrt{2}t_e$ arising from the possibility of two electrons tunneling [3]. Here, stronger electron-hole exchange ensures that effectively one electron spin is available for tunneling.

We next investigate the gate bias regime which allows us to switch the electron-hole interaction off through an optical double-resonance. This process is described in Fig. 3(b). Starting with an electron in the blue dot, the excitation of an indirect X^0 is followed by one of the electron tunneling to the back-contact as a two-electron charge in the blue QD is unstable at this gate bias, leaving a state with one electron in the blue and one hole in the red QD. This is the ground state of the X^{1+} transition which turns out to be at the same energy, which allows scattering until the hole tunnels out towards the top gate resetting the

system to the initial configuration of one electron in the blue dot. The relative brightness of the X^{1+} to the X^0 in Fig. 1(e) indicates that the lifetime of the optically generated hole is long compared to the lifetime of the exciton. Note that the indirect X^0 is comparatively weaker in the shown range. The electron-hole exchange interaction in the X^{1+} configuration will vanish because of the two holes in the red QD forming a singlet. Hence, the two lines in Fig. 3(a) effectively correspond to emission from an electronic singlet/triplet state formed by pure indirect electron-electron exchange (A similar two-electron coupling, but for the ground state was studied in Ref. [11]). Figure 3(b) shows the DT signal at a gate bias of 106.5 mV. By using a linearly polarized resonant laser, we find that the higher energy transmission dip that corresponds to the three triplet states has an area close to three times that of the lower energy one that corresponds to the singlet state. The splitting between the dips is about $8.5 \mu\text{eV}$. The electron tunneling rate corresponding to the measured splitting is found to be $t_e \approx 140 \mu\text{eV}$ which is close to the previously calculated value of $t_e = 137 \mu\text{eV}$ for CQD1.

Further in Fig. 3(c), we present data showing a strong polarization dependence of the two photon absorption process in Fig. 3(a). The resonance is clearly visible with linear polarized light, but with a circular polarized laser, it is substantially reduced. The optical selection rules for the indirect X^0 and the direct X^{1+} are orthogonal for circular polarization, thereby blocking either the optical charging of the hole or the scattering depending on the spin of the original electron in the blue QD.

In conclusion, we have demonstrated coherent coupling between two stacked QDs in the regime where the electron-hole exchange is the dominant interaction and leads to qualitative differences in the spectrum as compared to the case where the inter-dot indirect electron exchange process is the dominant scale. We were able to probe the opposite regime of nominally vanishing electron-hole exchange by varying the gate voltage and utilizing a double-resonance in absorption. We expect that the optical charge sensing that we used to identify the charging states in our system is itself a very valuable tool for other applications in quantum information processing such as single spin measurement via spin-charge conversion [12, 13].

Y. Z. wishes to acknowledge funding from LGFG. This work was supported by NCCR Quantum Photonics (NCCR QP), research instrument of the Swiss National Science Foundation (SNSF).

-
- [1] P. Michler, A. Kiraz, C. Becher, W. V. Schoenfeld, P. M. Petroff, L. Zhang, E. Hu, and A. Imamoglu, *Science* **290**, 2282 (2000).
- [2] S. Seidl, M. Kroner, P. A. Dalgarno, A. Hogele, J. M. Smith, M. Ediger, B. D. Gerardot, J. M. Garcia, P. M. Petroff, K. Karrai, et al., *Phys. Rev. B* **72**, 195339 (2005).
- [3] H. J. Krenner, M. Sabathil, E. C. Clark, A. Kress, D. Schuh, M. Bichler, G. Abstreiter, and J. J. Finley, *Phys. Rev. Lett.* **94**, 057402 (2005).
- [4] E. A. Stinaff, M. Scheibner, A. S. Bracker, I. V. Ponomarev, V. L. Korenev, M. E. Ware, M. F. Doty, T. L. Reinecke, and D. Gammon, *Science* **311**, 636 (2006).
- [5] M. Scheibner, M. F. Doty, I. V. Ponomarev, A. S. Bracker, E. A. Stinaff, V. L. Korenev, T. L. Reinecke, and D. Gammon, *Phys. Rev. B* **75**, 245318 (2007).
- [6] H. J. Krenner, E. C. Clark, T. Nakaoka, M. Bichler, C. Scheurer, G. Abstreiter, and J. J. Finley, *Phys. Rev. Lett.* **97**, 076403 (2006).
- [7] M. F. Doty, M. Scheibner, I. V. Ponomarev, E. A. Stinaff, A. S. Bracker, V. L. Korenev, T. L. Reinecke, and D. Gammon, *Phys. Rev. Lett.* **97**, 197202 (2006).
- [8] B. Alen, F. Bickel, K. Karrai, R. J. Warburton, and P. M. Petroff, *Appl. Phys. Lett.* **83**, 2235 (2003).
- [9] R. J. Warburton, C. Schäflein, F. B. D. Haft, A. Lorke, K. Karrai, J. M. Garcia, W. Schoenfeld, and P. M. Petroff, *Nature (London)* **405**, 926 (2000).
- [10] M. Ediger, P. A. Dalgarno, J. M. Smith, B. D. Gerardot, R. J. Warburton, K. Karrai, and P. M. Petroff, *Appl. Phys. Lett.* **86**, 211909 (2005).
- [11] H. E. Tureci, J. M. Taylor, and A. Imamoglu, *cond-mat/0611469* (2006).
- [12] M. Field, C. G. Smith, M. Pepper, D. A. Ritchie, J. E. F. Frost, G. A. C. Jones, and D. G. Hasko, *Phys. Rev. Lett.* **70**, 1311 (1993).
- [13] J. M. Elzerman, R. Hanson, L. H. W. van Beveren, B. Witkamp, L. M. K. Vandersypen, and L. P. Kouwenhoven, *Nature (London)* **430**, 431 (2004).
- [14] T. Nakaoka, T. Saito, J. Tatebayashi, and Y. Arakawa, *Phys. Rev. B* **70**, 235337 (2004).
- [15] The splitting of the red X^0 line in Fig. 2(c) would correspond to an exciton g-factor of only 0.6, which is the expected contribution from the electron. Considering the unusual energy of X^{+1} relative to X^0 , we could argue that the stacked QD has different shape and different strain

in and around the QD. These effects affects the hole g-factor more than the electron and the g-factor of the hole can even change sign [14]. The X^{-1} line of the blue QD has an exciton g-factor of 1.93.

- [16] The X^0 of the red CQD1 has the unusual attribute of an X-Y splitting that is less than the linewidth.